



Universiteit
Leiden
The Netherlands

Discovery of a Probable 4-5 Jupiter-mass Exoplanet to HD 95086 by Direct Imaging

Rameau, J.; Chauvin, G.; Lagrange, A.; Boccaletti, A.; Quanz, S.; Bonnefoy, M.; ... ; Kenworthy, M.

Citation

Rameau, J., Chauvin, G., Lagrange, A., Boccaletti, A., Quanz, S., Bonnefoy, M., ... Kenworthy, M. (2013). Discovery of a Probable 4-5 Jupiter-mass Exoplanet to HD 95086 by Direct Imaging. *The Astrophysical Journal Letters*, 772(2), L15. doi:10.1088/2041-8205/772/2/L15

Version: Publisher's Version

License: [Leiden University Non-exclusive license](#)

Downloaded from: <https://hdl.handle.net/1887/81342>

Note: To cite this publication please use the final published version (if applicable).

ERRATUM: “DISCOVERY OF A PROBABLE 4–5 JUPITER-MASS EXOPLANET TO
HD 95086 BY DIRECT-IMAGING” (2013, *ApJL*, 772, L15)

J. RAMEAU¹, G. CHAUVIN¹, A.-M. LAGRANGE¹, A. BOCCALETTI², S. P. QUANZ³, M. BONNEFOY⁴, J. H. GIRARD⁵, P. DELORME¹,
S. DESIDERA⁶, H. KLAHR⁴, C. MORDASINI⁴, C. DUMAS⁵, M. BONAVITA⁶, T. MESHKAT⁷, V. BAILEY⁸, AND M. KENWORTHY⁷

¹ UJF-Grenoble 1/CNRS-INSU, Institut de Planétologie et d’Astrophysique de Grenoble (IPAG) UMR 5274, F-38041 Grenoble, France

² LESIA, Observatoire de Paris, CNRS, University Pierre et Marie Curie Paris 6 and University Denis Diderot Paris 7, 5 place Jules Janssen, F-92195 Meudon, France

³ Institute for Astronomy, ETH Zurich, Wolfgang-Pauli-Strasse 27, 8093 Zurich, Switzerland

⁴ Max Planck Institute für Astronomy, Königstuhl 17, D-69117 Heidelberg, Germany

⁵ European Southern Observatory, Casilla 19001, Santiago 19, Chile

⁶ INAF-Osservatorio Astronomico di Padova, Vicolo dell’ Osservatorio 5, I-35122 Padova, Italy

⁷ Leiden Observatory, Leiden University, P.O. Box 9513, 2300 RA Leiden, The Netherlands

⁸ Steward Observatory, Department of Astronomy, University of Arizona, 933 North Cherry Avenue, Tucson, AZ 85721-0065, USA

Received 2013 July 22; published 2013 September 30

The erratum is issued because the published version omitted some contributors, these are: T. Meshkat, V. Bailey, and M. Kenworthy.

DISCOVERY OF A PROBABLE 4–5 JUPITER-MASS EXOPLANET TO HD 95086 BY DIRECT IMAGING*

J. RAMEAU¹, G. CHAUVIN¹, A.-M. LAGRANGE¹, A. BOCCALETTI², S. P. QUANZ³, M. BONNEFOY⁴, J. H. GIRARD⁵, P. DELORME¹,
S. DESIDERA⁶, H. KLAHR⁴, C. MORDASINI⁴, C. DUMAS⁵, AND M. BONAVITA⁶

¹ UJF-Grenoble 1/CNRS-INSU, Institut de Planétologie et d’Astrophysique de Grenoble (IPAG) UMR 5274, Grenoble F-38041, France;
julien.rameau@obs.ujf-grenoble.fr

² LESIA, Observatoire de Paris, CNRS, University Pierre et Marie Curie Paris 6 and University Denis Diderot Paris 7, 5 place Jules Janssen, F-92195 Meudon, France

³ Institute for Astronomy, ETH Zurich, Wolfgang-Pauli-Strasse 27, 8093 Zurich, Switzerland

⁴ Max Planck Institute for Astronomy, Königstuhl 17, D-69117 Heidelberg, Germany

⁵ European Southern Observatory, Casilla 19001, Santiago 19, Chile

⁶ INAF-Osservatorio Astronomico di Padova, Vicolo dell’ Osservatorio 5, I-35122 Padova, Italy

Received 2013 May 7; accepted 2013 May 24; published 2013 July 11

ABSTRACT

Direct imaging has only begun to inventory the population of gas giant planets on wide orbits around young stars in the solar neighborhood. Following this approach, we carried out a deep imaging survey in the near-infrared using VLT/NaCo to search for substellar companions. Here we report the discovery of a probable companion orbiting the young (10–17 Myr), dusty, early-type (A8) star HD 95086 at 56 AU in L' ($3.8 \mu\text{m}$) images. This discovery is based on observations with more than a year time lapse. Our first epoch clearly revealed the source at $\simeq 10\sigma$, while our second epoch lacks good observing conditions, yielding a $\simeq 3\sigma$ detection. Various tests were thus made to rule out possible artifacts. This recovery is consistent with the signal at the first epoch but requires cleaner confirmation. Nevertheless, our astrometric precision suggests that the companion is comoving with the star with a 3σ confidence level. The planetary nature of the source is reinforced by a non-detection in the Ks -band ($2.18 \mu\text{m}$) images according to its possible extremely red $Ks-L'$ color. Conversely, background contamination is rejected with good confidence level. The luminosity yields a predicted mass of about 4–5 M_{Jup} (at 10–17 Myr) using “hot-start” evolutionary models, making HD 95086 b the exoplanet with the lowest mass ever imaged around a star.

Key words: instrumentation: adaptive optics – planets and satellites: detection – stars: individual (HD 95086) – stars: massive

Online-only material: color figures

1. INTRODUCTION

Searching for orbiting giant planets by direct imaging is challenging due to the high planet–star contrast and the small angular separation explored. As a result, very few planetary-mass companions have been detected by direct imaging, initially at relatively large separations (≥ 100 AU) around solar-type to low-mass stars (e.g., Chauvin et al. 2005; Béjar et al. 2008; Lafrenière et al. 2008; Ireland et al. 2011). They may have a relatively high mass-ratio ($q \sim 0.2$ – 0.02), suggesting a stellar-like formation origin. More recently, the discoveries of giant planets around the young and dusty early-type stars HR 8799 (Marois et al. 2008, 2010) and β Pictoris (Lagrange et al. 2010) at smaller physical separations (≤ 70 AU) and with lower mass-ratio ($q \sim 0.002$) suggested rather a formation within the circumstellar disk either by core accretion (Pollack et al. 1996) or gravitational instability (Cameron 1978). Fomalhaut b (Kalas et al. 2008) is a particular case since its photometry seems to be contaminated by reflected light from dust (Currie et al. 2012), making the precise determination of its mass more uncertain. Also, the (proto-)planet candidates around LkCa 15 (Kraus & Ireland 2012) and HD 100546 (Quanz et al. 2013) still require confirmation. Consequently, every single discovery has a tremendous impact on the understanding of the formation, the dynamical evolution, and the physics of giant planets.

Although very few directly imaged giant planets, still very massive, have been reported in the literature, so far only one (maybe HR 8799 b, e.g., Marois et al. 2010) with a mass lower

than $7 M_{\text{Jup}}$ has been imaged around a star. Here we report the discovery of a probable 4–5 M_{Jup} giant planet around HD 95086, the exoplanet with the lowest mass ever imaged around a star. If the comoving status of the companion is confirmed, this giant planet may become a benchmark not only for physical studies of young giant planets but also for formation and evolution theories of planetary systems.

2. OBSERVATIONS AND DATA REDUCTION

2.1. The Star HD 95086

HD 95086 was identified as an early-type member of the Lower Centaurus Crux (LCC) association by de Zeeuw et al. (1999) and also by Madsen et al. (2002). The membership was established on the grounds that the star shares a similar velocity vector in the galactic framework as other LCC members. HD 95086 has a distance of 90.4 ± 3.4 pc (van Leeuwen 2007), which is approximately the mean distance of the LCC association. About the age of the association, Mamajek et al. (2002), followed by Pecaute et al. (2012), derived 17 ± 2 Myr (based on isochrone fitting), while Song et al. (2012) derived $\simeq 10$ Myr (by comparison with lithium equivalent width of members of other nearby associations). Systematic differences between these two fully independent methods may be responsible for the discrepancy. Nonetheless, the full assessment of the age is beyond the scope of this Letter and adopting 10 or 17 Myr only has a limited impact in the following results.

Houk & Cowley (1975) proposed that HD 95086 has a class III luminosity and an A8 spectral type with a mass of $\simeq 1.6 M_{\odot}$. However, its good-quality trigonometric parallax and thus derived luminosity and effective temperature undoubtedly

* Based on observations collected at the European Organisation for Astronomical Research in the Southern Hemisphere, Chile, under program Nos. 087.C-0292, 088.C.0085, 090.C-0538, 090.C-0698, and 090.C-0728.

Table 1
Observing Log of HD 95086 with VLT/NaCo

Type	Date	Cam./Filter	DIT × NDIT (s)	N_{exp}	π -start/End ($^{\circ}$)	(Airmass) ^a	(FWHM) ^a ($''$)	$\langle\tau_0\rangle^a$ (ms)	$\langle E_c\rangle^a$ (%)
θ_1 Ori C	2011 Dec 18	L27/L'	0.2×150	6	–/–	1.11	0.78	7.4	45.9
PSF	2012 Jan 11	L27/L'+ND	0.2×80	10	–9.32/–8.19	1.39	0.75	3.6	61.1
Deep	2012 Jan 11	L27/L'	0.2×100	156	–7.59/16.96	1.39	0.76	3.5	58.2
θ_1 Ori C	2012 Feb 10	L27/L'	0.2×195	10	–/–	1.06	0.50	6.0	37.1
PSF	2013 Feb 14	S13/Ks	0.2×100	4	–45.18/–44.72	1.52	1.08	1.1	54.5
Deep	2013 Feb 14	S13/Ks	0.5×100	88	–44.14/–14.68	1.45	1.08	1.1	22.4
θ_1 Ori C	2013 Mar 24	L27/L'	0.2×50	10	–/–	1.16	1.56	5.9	52.1
Deep	2013 Mar 14	L27/L'	0.2×100	162	3.20/28.18	1.41	1.77	1.0	37.2
PSF	2013 Mar 14	L27/L'+ND	0.2×80	10	29.61/30.68	1.44	1.65	0.9	32.1

Notes. “ND” refers to the NaCo ND_Long filter (transmission of $\simeq 1.79\%$), “PSF” to point-spread function for unsaturated exposures, “Deep” to deep science observations, “DIT” to exposure time, and π to the parallactic angle at the start and end of observations. θ_1 Ori C was observed in a field-stabilized mode.

^a The airmass, FWHM, coherence time τ_0 , and energy E_c are estimated in real time by the adaptive-optics system.

place it close to zero-age main-sequence stars of LCC and thus reject the supergiant phase.

Another interesting property of HD 95086 is that observations in the mm (Nilsson et al. 2010) and in the mid- to far-infrared (Rizzuto et al. 2012; Chen et al. 2012) revealed a large dust-to-star luminosity ratio ($L_d/L_* = 10^{-3}$), indicating the presence of a thus far unresolved debris disk.

Finally, Kouwenhoven et al. (2005) observed HD 95086 with adaptive optics and identified a background star with a separation of $4''.87$ and a position angle of 316° to the star (based on its K magnitude).

2.2. Observations

HD 95086 was observed with VLT/NaCo (Lenzen et al. 2003; Rousset et al. 2003) in thermal infrared and angular differential imaging (ADI; Marois et al. 2006) mode as part of our direct-imaging survey of young, dusty, early-type stars (Rameau et al. 2013). NaCo setups were the L' filter ($\lambda_0 = 3.8 \mu\text{m}$, $\Delta\lambda = 0.62 \mu\text{m}$) with the L27 camera in service mode for observations in 2012 January. The source was dithered within the instrument field of view ($\simeq 14'' \times 14''$) in order to properly estimate and remove the background contribution. An observing sequence was made up of a first short set of unsaturated exposures to serve as calibrations for the point-spread function (PSF) and for the relative photometry and astrometry. The sequence was followed by a one-hour set of deep science observations.

In 2013, follow-up observations were performed and included two runs: one in February (back-up star, visitor mode, very bad conditions) with the Ks filter ($\lambda_0 = 2.18 \mu\text{m}$, $\Delta\lambda = 0.35 \mu\text{m}$) and the S13 camera (plate scale $\simeq 13.25 \text{ mas pixel}^{-1}$), and one in March at L' with the L27 camera in service mode. Table 1 summarizes the observing log for each run. We recall that HD 95086 has $V = 7.36 \pm 0.01 \text{ mag}$, $Ks = 6.79 \pm 0.02 \text{ mag}$, and $6.70 \pm 0.04 \text{ mag}$ at $3.4 \mu\text{m}$ from the *WISE* database.

Finally, an astrometric calibrator, the θ_1 Ori C field, was observed for each observing run.

2.3. Data Reduction

Data reduction (flat-fielding, bad pixel and sky removal, registration,⁷ and image selection) was performed using the IPAG-ADI pipeline (e.g., Lagrange et al. 2010; Chauvin et al.

2012; Rameau et al. 2013 and references therein). Stellar-halo subtraction was also done using all the ADI algorithms implemented in the pipeline: cADI, sADI (Marois et al. 2006), and LOCI (Lafrenière et al. 2007). The frames were finally de-rotated and mean-combined. The astrometry and photometry of any detected point source as well as their error estimates were done similarly to Chauvin et al. (2012) and Lagrange et al. (2012) by injecting fake planets using the unsaturated PSF reduced images. The noise per pixel was derived from the standard deviation calculated in a ring of 1.5 FWHM width, centered on the star, with a radius of the separation of the source and masking the point-source itself. The flux of the point source was integrated over an aperture of 1.5 FWHM in diameter. The final signal-to-noise ratio (S/N) was then calculated on the same aperture size considering the noise per pixel and the aperture size in pixels.

The θ_1 Ori C field data were reduced for detector calibrations by comparison with *Hubble Space Telescope* observations by McCaughrean & Stauffer (1994; using the same set of stars TCC0051, 034, 029, and 026 at each epoch). We found, for the 2012 and 2013 data, a true north of $-0.37 \text{ deg} \pm 0.02 \text{ deg}$, $-0.38 \text{ deg} \pm 0.03 \text{ deg}$, and $-0.45 \text{ deg} \pm 0.09 \text{ deg}$, respectively, and a plate scale of $27.11 \pm 0.06 \text{ mas}$, $27.10 \pm 0.03 \text{ mas}$, and $27.10 \pm 0.04 \text{ mas}$, respectively.

Finally, the detection performance was derived by measuring the 5σ level noise in a sliding box of 5×5 pixels toward the direction of the point source and corrected for flux loss. The contrast was converted to mass with the “hot-start” COND models of Baraffe et al. (2003).

Two independent pipelines (Boccaletti et al. 2012; Amara & Quanz 2012) were also used for consistency and error estimates.

3. A COMPANION CANDIDATE AND A BACKGROUND STAR

3.1. Astrometry

The data in 2012 January showed the background star detected by Kouwenhoven et al. (2005) at a projected separation of $4''.540 \pm 0''.015$ from the central star and a position angle of $319.03 \text{ deg} \pm 0.25 \text{ deg}$ (see Figure 1, right panel). We also detected an additional, fainter signal southeast of the star with a S/N of 9. The robustness of this detection was strengthened due to its systematic confirmation via the mean of a series of tests using three independent pipelines, all our published flavors of ADI algorithms, and an extensive parameter space exploration.

⁷ The central star was not saturated in the deep science observations; this enabled us to get very good accuracy on the measurements of the star position using Moffat fittings.

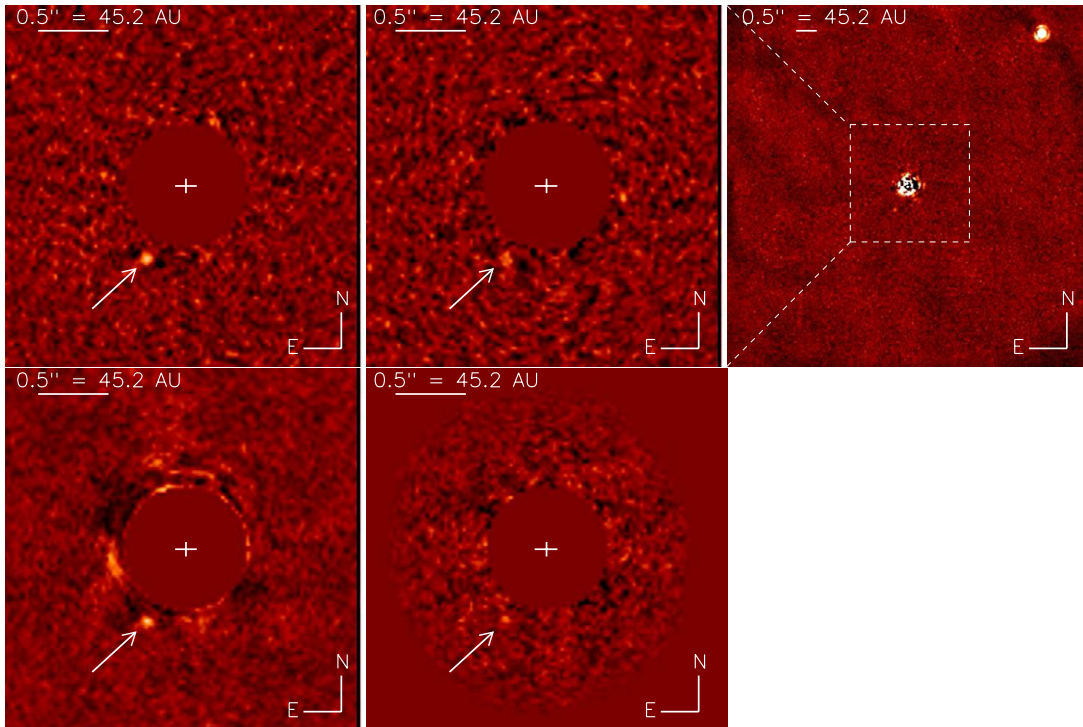


Figure 1. Residual maps (sADI at top and LOCI at bottom) at L' showing the companion candidate in 2012 (left) with an S/N of 9 and in 2013 (middle) with an S/N of 3. Top right: larger field of view with the visual binary at northwest in 2012. Bright residuals are remaining speckles from the Airy ring at the same separation of the companion candidate.

(A color version of this figure is available in the online journal.)

The source successfully passed all tests. The top and bottom left panels of Figure 1 represent the companion candidate (CC) located at a separation of 623.9 ± 7.4 mas and a position angle of $151.8 \text{ deg} \pm 0.8 \text{ deg}$ from the central star, using the sADI algorithm (with 20 frames combined for $N_\delta = 1$ (FWHM) at $r = 540''$) and LOCI (with $N_\delta = 0.75$ (FWHM), $dr = 3$ (FWHM), $g = 1$, and $N_A = 300$ (FWHM)), respectively.

With HD 95086 being at very low galactic latitude ($b \simeq -8^\circ$), the contamination by background objects is relatively high, even at L' . A time lapse long enough with another data set was mandatory to prove the companionship of each object (see Section 4.1).

In the 2013 L' data, both objects were detected at similar locations as in 2012. However, the weather conditions strongly varied over the sequence, thereby revealing the CC with a lower S/N of 3. We carried out the same tests as for the 2012 data for this data set and the CC was detected. The signal is thus consistent with the object seen in 2012, even at low S/N. The residual map with the CC southeast from the star is displayed in the top and bottom middle panels of Figure 1 using sADI with the 2012 parameters and LOCI with $N_\delta = 0.75$ (FWHM), $dr = 1$ (FWHM), $g = 0.5$, and $N_A = 600$ (FWHM). The positions are 626.11 ± 12.8 mas and $150.7 \text{ deg} \pm 1.3 \text{ deg}$ for the separation and position angle of the CC, and $4''.505 \pm 0''.016$ and $319.42 \text{ deg} \pm 0.26 \text{ deg}$ for the background star.

At Ks , we did not detect the CC (Figure 2, bottom left panel). Conversely, the background star was revealed, as well as seven other point sources not seen at L' . This may be consistent with background objects.

3.2. Photometry

In the 2012 L' data, we derived the star-to-CC contrast to be $9.79 \pm 0.40 \text{ mag}$ ($L' = 16.49 \pm 0.50 \text{ mag}$) and $6.2 \pm 0.2 \text{ mag}$

for the background star. The error budget includes, from high-to-low significance, photometry of the CC, neutral density, PSF flux estimate, and variability. Similar results have been obtained with other algorithms and pipelines. In the 2013 L' data, the weakness of the CC signal impacted the estimation of the photometry and higher uncertainties than in 2012 data, but the L' contrast was consistent and of $9.71 \pm 0.56 \text{ mag}$. For the background star, we found $\Delta L' = 6.1 \pm 0.2 \text{ mag}$.

Finally, at Ks , we estimated $\Delta Ks = 5.84 \pm 0.1 \text{ mag}$ for the background star. The non-detection of the CC directly also provided an upper limit to the $Ks-L'$ color of 1.2 mag.

4. DISCUSSION

In the following, we discuss the nature of the two detected objects at HD 95086 as well as their physical properties.

4.1. Background Objects?

HD 95086 has a proper motion of $[-41.41 \pm 0.42, 12.47 \pm 0.36] \text{ mas yr}^{-1}$ and a parallax of $11.06 \pm 0.41 \text{ mas}$ (van Leeuwen 2007), hence translating into an amplitude of $58.886 \pm 0.002 \text{ mas}$ (more than 2 NaCo/L27 pixels) between the two epochs. Figure 2 (top left) shows that the northwestern star is unambiguously of background, based on astrometric measurements rather than on photometric ones (Kouwenhoven et al. 2005). This analysis strengthened our capability to discriminate between background behavior and common proper motion with the parent star, despite the relatively low amplitude between the two epochs.

Figure 2 (top right) presents the sky relative positions for the CC. Its background nature may be excluded with a χ^2 probability of 3×10^{-3} (3σ confidence level). For further

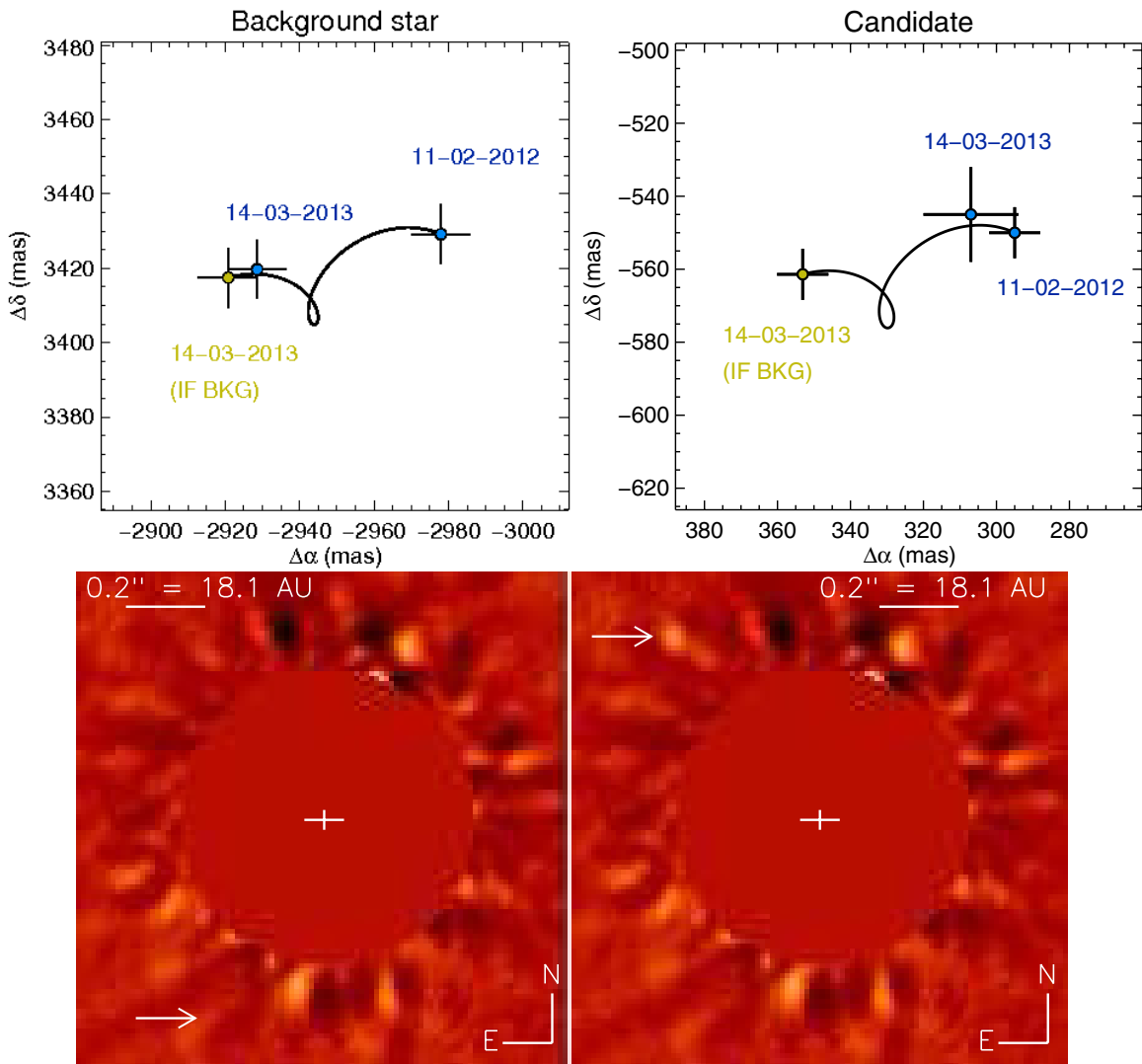


Figure 2. Top right: relative separations between the central star and a candidate companion in right ascension (α) and declination (δ). The epoch-one astrometric point is plotted in blue (2012 January 11) and linked to the expected position of the CC, if it were a background object (gold, 2013 March 14), by a proper and parallactic motion track. The epoch-two astrometric point in 2013 is overplotted in blue. This is the case of the CC, which may be inconsistent with a background status (at the 3σ confidence level). Top left: case of the northwestern background star. Bottom: residual maps (sADI) at K_s showing the non-detection of the CC in 2013 (left) and the recovery of an M-dwarf contaminant with $K_s-L' \simeq 0.4$ if located at the same separation as the CC (right). Speckles and residuals at the same separation as the CC, or closer in, are due to spiders and poor PSF subtraction.

(A color version of this figure is available in the online journal.)

investigations of the background hypothesis, we ran simulations with the Besançon galactic model (Robin et al. 2003) to identify the probability of contamination by stars with $L' \simeq 17$ mag and their properties. We found that in a field of view of radius $1''$ around HD 95086, this probability is about 0.11% and dominated by M dwarfs (peak at $K_s = 19$ mag). Making the assumption of an M-type background star, the resulting $K_s-L' \simeq 0.4$ color would imply $K_s \simeq 16.9$ mag, which would easily be detected in our observations. Therefore, we injected a PSF scaled to the flux into the K_s data at the separation of the CC and reduced within the pipeline. The signal was unveiled with a S/N of 15 (see Figure 2, bottom right). As a result, the K_s data set should have exhibited the CC if it had been the reddest contaminant even though the observing conditions were bad. For these reasons, background contamination by a late-K to M dwarf seems improbable and only a very red object (planet, brown dwarf) may match the K_s-L' constraint. Finally, according to Delorme et al. (2010), the probability of

finding a fore/background field L or T dwarf around HD 95086 ($1''$ radius) down to $L' \leq 17$ mag is about 10^{-5} .

From both astrometry and photometry points of view, we conclude that a contamination appears very unlikely.

4.2. Physical Properties of the Candidate Companion and Additional Planets

In the following, we assume that the CC is a bound companion hereafter named HD 95086 b.

First, the measured separation of 623.9 ± 7.4 mas of HD 95086 b (from the 2012 data with the highest S/N) translates into a projected distance of 56.4 ± 0.7 AU.

Given the observed contrast ($\Delta L' = 9.79 \pm 0.40$ mag), distance (90.4 ± 3.4 pc), and HD 95086 magnitude (6.70 ± 0.09), we derived $M_{L'} = 11.71 \pm 0.53$ mag for HD 95086 b. This translates, according to the COND evolutionary model (Baraffe et al. 2003), into a mass of $5 \pm 1 M_{\text{Jup}}$ at 17 ± 2 Myr and

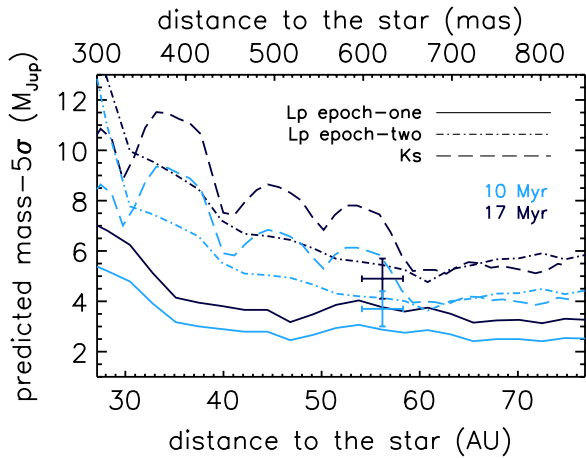


Figure 3. 5σ detection limits with sADI, toward the direction of the CC in mass vs. separation for each epoch in L' (solid, 2012, and dash-dotted, 2013, lines) and Ks (dashed line). Limits have been derived for an age of 17 Myr (light color) and 10 Myr (dark color) from COND models. The CC properties have been overplotted at each age. Note that for the second epoch in L' , it is detectable at a S/N of 3 only, thus below the limit here. We also see from the Ks performance that the CC is indeed not detectable.

(A color version of this figure is available in the online journal.)

$4 \pm 1 M_{\text{Jup}}$ at 10 Myr. We checked that, given such a mass, HD 95086 b cannot be detected at Ks . Figure 3 displays L' 5σ -detection performances toward the direction of HD 95086 b. Our sensitivity ruled out any additional companion as light as $4 M_{\text{Jup}}$ from 48 AU and 1200 AU. The presence of any planet more massive than $8 M_{\text{Jup}}$ and $12 M_{\text{Jup}}$ can be excluded beyond 38 AU and 34 AU, respectively, in projected separation. Moreover, we attempted a comparison of the L' -band magnitude of HD 95086 b to “warm-start” evolutionary models’ predictions (Spiegel & Burrows 2012) with different initial conditions (see Figure 11 of Bonnefoy et al. 2013). We found a mass greater than $3 M_{\text{Jup}}$ using the youngest age estimate of the system and three-times solar metallicity hybrid cloud models. The lack of prediction for $M \geq 15 M_{\text{Jup}}$ prevented us from giving an upper limit of the mass.

Lastly, Figure 4 compares the HD 95086 b magnitude and color upper limit with those of other companions, field dwarfs, and tracks from COND and DUSTY evolutionary models (Baraffe et al. 2003; Chabrier et al. 2000). HD 95086 b, HR 8799 cde, and 2M 1207 b appear to be similar in the sense that they all lie at the L–T transition and are less luminous than all other companions except HR 8799 b. The Ks – L' limit suggests that HD 95086 b is at least as cool as HR 8799 cde and 2M 1207 b (Chauvin et al. 2004). Moreover, with a predicted temperature estimate of 1000 ± 200 K and $\log g$ of 3.85 ± 0.5 derived from the L' magnitude, HD 95086 b would enable us to further explore the impact of reduced surface gravity on the strength of methane bands in the near-infrared.

4.3. Concluding Remarks

We reported the probable discovery of the exoplanet HD 95086 b, which may be the planet with the lowest mass ever imaged around a star.

In a nutshell, our L' observations revealed the probable planet in 2012 with a S/N of 10 and the likely re-detection of it in 2013 at a S/N of 3. It is separated from its host star by 56.4 ± 0.7 AU in projection, has $L' = 16.49 \pm 0.50$ mag, and an upper limit for the Ks – L' color of 1.2 mag from the non-detection at Ks . These Ks observations also allowed us to reject the background

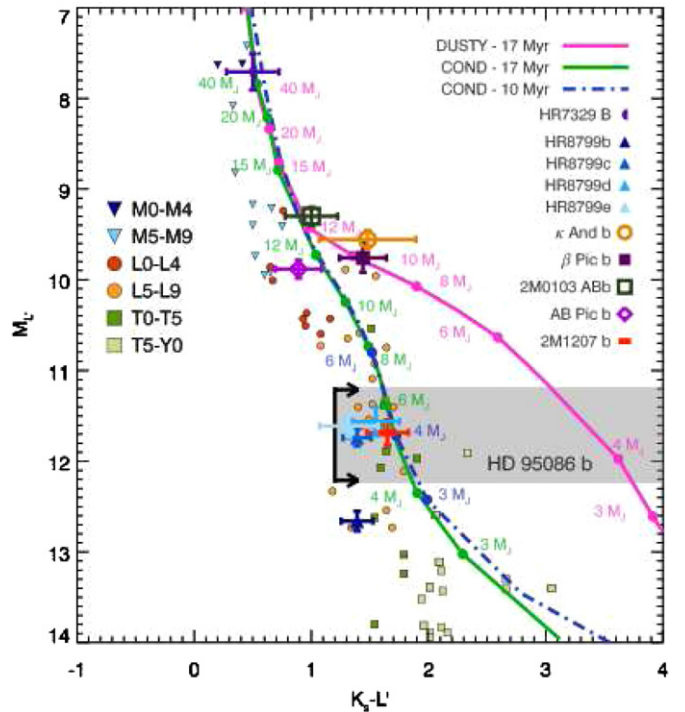


Figure 4. $M_{L'}$ vs. Ks – L' magnitude–color diagram. The location of HD 95086 b with the upper limit at Ks is shown with the shaded region with respect to field M (triangles), L (circles), and T (squares) dwarfs (Leggett et al. 2013). The colors of young substellar companions are overlaid as well as COND and DUSTY evolutionary tracks at 10 Myr (dash-dotted line) and 17 Myr (solid lines).

(A color version of this figure is available in the online journal.)

hypothesis by the most probable contaminants that would have been detected. In addition, we emphasized the comoving status of the planet with a 3σ confidence level based on our astrometric measurements in 2012 and 2013. Another data set such as the one in 2012 with $S/N \geq 5$ would significantly improve the astrometric precision and thus ascertain the bound status. Finally, we derived a mass of 4 ± 1 to $5 \pm 1 M_{\text{Jup}}$ for HD 95086 b using the COND models and an age of $\simeq 10$ or 17 ± 2 Myr for the system.

HD 95086, having a large infrared excess, and its probable planet, likely having $q \simeq 0.002$, lend support to the assumption that HD 95086 b formed within the circumstellar disk like β Pic b or HR 8799 bcde. Regarding the separation, HD 95086 b has a projected physical separation about 56 AU, which is very similar to the brown dwarf κ And b (Carson et al. 2013) which is smaller than that of HR 8799 b but larger than those of c and d, and much larger than β Pictoris and HR 8799 e. Therefore, this giant planet may also be challenging for the classical formation mechanisms, specifically for core accretion. The timescale to reach the critical core mass of $10 M_{\oplus}$ for gas accretion is far longer than the gas dispersal one (from 10^6 to 10^7 Myr) and thus inhibits the in situ formation of a giant planet beyond very few tens of AU (Rafikov 2011). Particular circumstances for core accretion (Kenyon & Bromley 2009) or an alternative scenario such as pebble accretion (Lambrechts & Johansen 2012) may occur instead. Another possible mechanism is gravitational instability. At 56 AU, the fragmentation of the protostellar disk of HD 95086 ($1.6 M_{\odot}$) can occur (Dodson-Robinson et al. 2009), but such a low mass planet might not be formed through direct collapse. It may result from subsequent clump fragmentation or from gravitational instability with peculiar disk properties (Kratter et al. 2010). Finally, there is also the

possibility that HD 95086 b was formed closer to the star by core accretion and migrated outward due to interactions with the disk or planet–planet scattering (Crida et al. 2009) to its current position. Orbital monitoring showing eccentricity would likely ascertain the presence of an unseen close-in, higher mass planet.

Future observations with NaCo and next planet imagers will be important for providing new photometric points at predicted $H \simeq 18.9$ mag and $K \simeq 18.5$ mag to further explore its atmosphere properties and to search for additional close-in planets.

This research has made use of the SIMBAD database operated at CDS, Strasbourg, France, and of the NASA/IPAC Infrared Science Archive, which is operated by the Jet Propulsion Laboratory, California Institute of Technology, under contract with the National Aeronautics and Space Administration. J.R., G.C., A.-M.L., and P.D. also acknowledge financial support from the French National Research Agency (ANR) through project grant ANR10-BLANC0504-01. S.D. acknowledges partial support from PRIN INAF 2010 planetary systems at young ages.

Facility: VLT:Yepun (NaCo)

REFERENCES

- Amara, A., & Quanz, S. P. 2012, *MNRAS*, **427**, 948
- Baraffé, I., Chabrier, G., Barman, T. S., Allard, F., & Hauschildt, P. H. 2003, *A&A*, **402**, 701
- Béjar, V. J. S., Zapatero Osorio, M. R., Pérez-Garrido, A., et al. 2008, *ApJL*, **673**, L185
- Boccaletti, A., Augereau, J.-C., Lagrange, A.-M., et al. 2012, *A&A*, **544**, A85
- Bonnefoy, M., Boccaletti, A., Lagrange, A.-M., et al. 2013, *A&A*, in press (arXiv:1302.1160)
- Cameron, A. G. W. 1978, *M&P*, **18**, 5
- Carson, J., Thalmann, C., Janson, M., et al. 2013, *ApJL*, **763**, L32
- Chabrier, G., Baraffe, I., Allard, F., & Hauschildt, P. 2000, *ApJ*, **542**, 464
- Chauvin, G., Lagrange, A.-M., Beust, H., et al. 2012, *A&A*, **542**, A41
- Chauvin, G., Lagrange, A.-M., Dumas, C., et al. 2004, *A&A*, **425**, L29
- Chauvin, G., Lagrange, A.-M., Zuckerman, B., et al. 2005, *A&A*, **438**, L29
- Chen, C. H., Pecaute, M., Mamajek, E. E., Su, K. Y. L., & Bitner, M. 2012, *ApJ*, **756**, 133
- Crida, A., Masset, F., & Morbidelli, A. 2009, *ApJL*, **705**, L148
- Currie, T., Debes, J., Rodigas, T. J., et al. 2012, *ApJL*, **760**, L32
- Delorme, P., Albert, L., Forveille, T., et al. 2010, *A&A*, **518**, A39
- de Zeeuw, P. T., Hoogerwerf, R., de Bruijne, J. H. J., Brown, A. G. A., & Blaauw, A. 1999, *AJ*, **117**, 354
- Dodson-Robinson, S. E., Veras, D., Ford, E. B., & Beichman, C. A. 2009, *ApJ*, **707**, 79
- Houk, N., & Cowley, A. P. 1975, University of Michigan Catalogue of Two-dimensional Spectral Types for the HD Stars, Vol. I (Ann Arbor, MI: Department of Astronomy, Univ. Michigan)
- Ireland, M. J., Kraus, A., Martinache, F., Law, N., & Hillenbrand, L. A. 2011, *ApJ*, **726**, 113
- Kalas, P., Graham, J. R., Chiang, E., et al. 2008, *Sci*, **322**, 1345
- Kenyon, S. J., & Bromley, B. C. 2009, *ApJL*, **690**, L140
- Kouwenhoven, M. B. N., Brown, A. G. A., Zinnecker, H., Kaper, L., & Portegies Zwart, S. F. 2005, *A&A*, **430**, 137
- Kratter, K. M., Murray-Clay, R. A., & Youdin, A. N. 2010, *ApJ*, **710**, 1375
- Kraus, A. L., & Ireland, M. J. 2012, *ApJ*, **745**, 5
- Lafrenière, D., Jayawardhana, R., & van Kerkwijk, M. H. 2008, *ApJL*, **689**, L153
- Lafrenière, D., Marois, C., Doyon, R., Nadeau, D., & Artigau, É. 2007, *ApJ*, **660**, 770
- Lagrange, A.-M., Boccaletti, A., Milli, J., et al. 2012, *A&A*, **542**, A40
- Lagrange, A.-M., Bonnefoy, M., Chauvin, G., et al. 2010, *Sci*, **329**, 57
- Lambrechts, M., & Johansen, A. 2012, *A&A*, **544**, A32
- Leggett, S. K., Morley, C. V., Marley, M. S., et al. 2013, *ApJ*, **763**, 130
- Lenzen, R., Hartung, M., Brandner, W., et al. 2003, *Proc. SPIE*, **4841**, 944
- Madsen, S., Dravins, D., & Lindegren, L. 2002, *A&A*, **381**, 446
- Mamajek, E. E., Meyer, M. R., & Liebert, J. W. 2002, *BAAS*, **34**, 762
- Marois, C., Lafrenière, D., Doyon, R., Macintosh, B., & Nadeau, D. 2006, *ApJ*, **641**, 556
- Marois, C., Macintosh, B., Barman, T., et al. 2008, *Sci*, **322**, 1348
- Marois, C., Zuckerman, B., Konopacky, Q. M., Macintosh, B., & Barman, T. 2010, *Natur*, **468**, 1080
- McCaughrean, M. J., & Stauffer, J. R. 1994, *AJ*, **108**, 1382
- Nilsson, R., Liseau, R., Brandeker, A., et al. 2010, *A&A*, **518**, A40
- Pecaute, M. J., Mamajek, E. E., & Bubar, E. J. 2012, *ApJ*, **746**, 154
- Pollack, J. B., Hubickyj, O., Bodenheimer, P., et al. 1996, *Icar*, **124**, 62
- Quanz, S. P., Amara, A., Meyer, M. R., et al. 2013, *ApJL*, **766**, L1
- Rafikov, R. R. 2011, *ApJ*, **727**, 86
- Rameau, J., Chauvin, G., Lagrange, A.-M., et al. 2013, *A&A*, **553**, A60
- Rizzuto, A. C., Ireland, M. J., & Zucker, D. B. 2012, *MNRAS*, **421**, L97
- Robin, A. C., Reylé, C., Derrière, S., & Picaud, S. 2003, *A&A*, **409**, 523
- Rousset, G., Lacombe, F., Puget, P., et al. 2003, *Proc. SPIE*, **4839**, 140
- Song, I., Zuckerman, B., & Bessell, M. S. 2012, *AJ*, **144**, 8
- Spiegel, D. S., & Burrows, A. 2012, *ApJ*, **745**, 174
- van Leeuwen, F. 2007, *A&A*, **474**, 653